Biochimica et Biophysica Acta, 722 (1983) 480–491
Elsevier Biomedical Press

BBA 41265

PHASE FLUORIMETRIC LIFETIME SPECTRA

I. IN ALGAL CELLS AT 77 K

ISMAEL MOYA and RAPHAEL GARCIA

Laboratoire de Photosynthèse, C.N.R.S., 91190 Gif-sur-Yvette (France)

(Received November 19th, 1982)

Key words: Fluorescence lifetime; Phase fluorimetry; Photosynthesis; (Alga)

A new method for decomposing fluorescence emission spectra into their elementary components, based on the simultaneous recording of fluorescence intensity and lifetime vs. the emission wavelength, has been applied to the spectra of algal cells at liquid nitrogen temperature. A model of Gaussian components fits both $\tau(\lambda)$ and $F(\lambda)$ spectra with the same parameters. The fluorescence lifetimes have been measured by phase fluorimetry at two modulation frequencies: 29 and 139 MHz. The final Gaussian decomposition is able to describe both the 29 and 139 MHz spectra. The following conclusions concerning the fluorescence spectra of *Chlorella* cells at 77 K can be drawn. These conclusions are also valid with minor changes for the other examined species. (1) An overlapping of different emitting bands occurs in all the spectra; therefore, a direct lifetime reading from phase delay measurement necessitates measurements being made at several frequencies. (2) At the F_{max} fluorescence level, the lifetime values of the two emissions usually associated with variable fluorescence are 0.53 ns (for B_1'; λ peak 688 nm), and 1.46 ns (for B_2'; λ peak 698 nm); these lifetimes are shorter than those we have measured at room temperature (approx. 1.8 ns). (3) Superimposed on B_1' and B_2' and with approximatively the same peak location, two long-lifetime components (B_1'', 4.8 ns; B_2'', 5.6 ns) are present. Two hypotheses can be proposed to explain these emissions: (i) the long-lifetime components arise from subsets of chlorophyll *a* disconnected from the functional antenna by the cooling process; and (ii) charge recombination in reaction centers leads to delayed fluorescence. (4) In the $\lambda > 710$ nm region, two main bands are required to describe the so-called Photosystem I emission: B_3 (0.8 ns; λ peak 715 nm) and B_4 (3.3 ns; λ peak 724 nm). The former band, usually unresolved in the amplitude fluorescence spectra, is a specific finding from lifetime measurements and has been associated with the antenna core of Photosystem I. No additional information has been obtained for B_4. A supplementary small band (B_5, 0.40 ns; λ peak $\simeq$ 740 nm) is necessary to take into account the frequency effect and the $\tau(\lambda)$ decrease in the $\lambda > 740$ nm spectral range.

Introduction

Investigation of the spectral properties of photosynthetic material at low temperature using fluorescence techniques began in the late fifties [1]. The discovery of the long-wave emission band (720 nm in *Chlorella* at 77 K) by Brody [2] firmly established the techniques. In the following decades, Butler et al. [3], Cho and Govindjee [4], Harnischfeger [5], Litvin et al. [6], Rijgersberg et al. [7] and others have contributed to the description of the low-temperature spectra (for reviews, see Refs. 8–10). The theoretical work of Paillotin

Abbreviations: Chl, chlorophyll; PS, photosystem.

[11] established the predictions of the temperature effect on the fluorescence parameters.

These predictions are in good agreement with the well known spectral characteristics of low-temperature fluorescence:

Compared to room temperature, the total fluorescence is increased by a factor of 4–10 [4]; this large enhancement is mainly due to the quantum yield increase of weakly fluorescent bands at room temperature, as we show later.

The emission spectrum shows at least three well defined bands [12]. The peak location can change with species: in *Chlorella,* F-689 and F-699 are sensitized by Chl *b* and are attributed to PS II [4]. The broad F_1 band (peak at 720 nm) is preferentially excited by Chl *a* and is attributed to PS I.

At low temperature the electron flow between Q (the primary quinone acceptor of PS II) and A (secondary plastoquinone acceptor) is blocked but the fluorescence induction curve is not photochemical because the reaction is limited by the electron donation to $P\text{-}680^+$ [12]. The extent of the fluorescence transient for dark-adapted algae, cooled in the dark, depends greatly on the wavelength emission. For F-689 and F-699 bands, the amplitude of the fluorescence transient is of the same order of magnitude as that at room temperature: $2 < F_{max}/F_{initial} < 4$, but for the broad F_1 band the ratio $F_{max}/F_{initial}$ is only 1.2–1.5 [3].

The induction kinetics at 77 K have been analysed by several authors [14–23]. Butler and Strasser [21] have developed a very complete model ('tripartite model') of the photosynthetic apparatus based on quantitative measurements of constant and variable fluorescence at two wavelengths: 692 and 730 nm. These authors assume that F-692 is mainly a PS II emission, and F-730 mainly a PS I emission: the variable fluorescence at 730 nm comes from energy transfer from PS II to PS I. Assuming that only the physical relationship between PS II and PS I is affected by cations like Mg^{2+}, Butler and co-workers can calculate changes of the transfer rate (spillover) induced by Mg^{2+} addition and the subsequent change of the initial energy redistribution between the two photosystems.

There is no doubt that the 'bipartite' and tripartite models can be a helpful tool in providing a rough picture of primary processes taking place at low temperature. Nevertheless, the data derived from fluorescence intensity measurements are not sufficient to resolve the evident complexity of low-temperature fluorescence. This points out the necessity of knowing the other parameters of fluorescence such as lifetime or polarisation as has recently been attempted [24,25].

Data published for low-temperature lifetime measurements

Lifetime data at 77 K are summarized in Table I [26–37]. It is difficult to obtain a clear picture of this problem for several different reasons:

disparity in the use of various photosynthetic systems (algae, chloroplasts or subchloroplasts particles);

disparity in the method employed to measure lifetimes (phase fluorimetry, photon counting or picosecond pulses);

large differences in the intensity employed; this difference is tremendous between the phase or counting method and the pulse method, but can also exist between experiments using a single pulse or the full train generated by the mode-locked lasers;

diversity of the excitation wavelengths (picosecond data of Table I are obtained with 530 nm excitation); and

disparity in the spectral band analyzed; nevertheless, it seems that lifetimes measured at short wavelengths are shorter (approx. 1–2 ns) than those measured at long wavelengths (approx. 2–3 ns).

Hervo et al. [28], based on their data with photon-counting techniques, suggested that F-730 (and also F-680) are multicomponent emissions. This conclusion is in good agreement with the heterogeneous character of the 77 K fluorescence spectrum which shows considerable overlap of the different bands, and leads us to the question as to whether picosecond experiments can resolve such multiexponential decays.

Our greatest interest was to know the mean value of the lifetime at each emission wavelength in order to time-resolve the emission spectrum. To perform this task, only one method can provide enough temporal resolution (5–10 ps) at a high data acquisition rate (approx. 20 ms): and this method is phase fluorimetry.

TABLE I

Authors	Material	$\lambda_{exc.}$ (nm)	$\lambda_{anal.}$ (nm)	τ (ns)	Intensity	Method	Observations
Butler and Norris [26]	pea leaf	blue	> 720	3.1 ± 0.1	low	phase fluorimetry	
Mar and co-workers [27]	*Chlorella* cells	632.8	685 730	1.4 2.3	low	phase fluorimetry	75 MHz mode-locked HeNe laser
Hervo and co-workers [28]	spinach chloroplasts	blue wide band	680	0.9 7	very low	photon counting	multiexponential decay
				0.9			
			730	1.5 5			
Harris and co-workers [29]	*Chlorella* cells	530	691 > 715	2.46	single pulse 10^{14} $h\nu$/cm^2 or full train	picosecond pulses + streak camera	τ independent of analysis wavelength Decays described by $I(t) = I_0 \exp[-(At + B\sqrt{t})]$
Searle and co-workers [30]	stroma PS I particles	530	> 665 > 720	1.82	single pulse $> 5 \cdot 10^{13}$ $h\nu$/cm^2	picosecond pulses + streak camera	–
	grana PS I particles	530	> 720	1.9			
	PS II particles (digitonin)	530	> 665	2.47			
Porter and co-workers [31]	*Chlorella* cells	530	> 665	2.8	single pulse $3 \cdot 10^{13}$ $h\nu$/cm^2	picosecond pulses + streak camera	evidence of intensity effects at high excitation intensities
		530	> 665	0.43	$8 \cdot 10^{15}$ $h\nu$/cm^2		
Yu and co-workers [32]	spinach chloroplasts	530	685	0.045 0.22	$2 \cdot 10^{14}$ $h\nu$/cm^2 by pulse	train of 100-ps pulses + ultra-fast Kerr shutter technique	90 K
			695 730	0.22 0.6			
Geacintov and co-workers [33]	chloroplasts	530	685	0.7	single pulse $2.5 \cdot 10^{14}$ $h\nu$/cm^2	picosecond pulses + streak camera	τ_{730} does not depend on excitation intensity
			730	1.1			

TABLE I (continued)

Authors	Material	$\lambda_{exc.}$ (nm)	$\lambda_{anal.}$ (nm)	τ (ns)	Intensity	Method	Observations
Campillo and co-workers [34]	Spinach chloroplasts	530	690	0.9	single pulse $2 \cdot 10^{14}$ $h\nu/cm^2$	picosecond pulses + streak camera	$\approx$ 140 ps delay on the rise of F-730
Rubin and Rubin [35]	pea chloroplasts	530	680 730	$\approx$ 1.3 $\approx$ 2.4	single pulse $5 \cdot 10^{12}$ $h\nu/cm^2$	picosecond pulses + streak camera	τ_{730} is intensity dependent
Butler and co-workers [36]	pea chloroplasts	530	715	2	single pulse $2 \cdot 10^{14}$ $h\nu/cm^2$	picosecond pulses + streak camera	monoexponential decay absence of delay of τ ($\lambda > 715$ nm) same lifetime for F(P) and F(o)
Wong and co-workers [37]	sucrose-washed pea chloroplasts + 10 mM NaCl + 10 mM $MgCl_2$	632.8	686 695 730 686 695 730	0.4 0.8 2.14 0.6 1.0 2.1	low	phase fluorimetry at 75 MHz	single-frequency experiments

Material and Methods

The samples used included unicellular green algae (*Chlorella pyrenoidosa, Chlamydomonas reinhardii, Euglena gracilis*) and a blue alga (*Aphanocapsa*), grown as described elsewhere [38,39]. The green alga *Ulva lactuca* was harvested on the coast of the Chausey Islands and kept in seawater for a few days.

The principle of phase fluorimetry is well known [40–45]. The main difficulty is to modulate the excitation source at a frequency (ν) in the same range of $(2\pi\tau)^{-1}$ (τ, fluorescence lifetime). The resulting fluorescence is also modulated at the same frequency and phase shifted by an angle ψ given by $\tan\psi = 2\pi\nu\tau$; the a.c. fluorescence component at frequency ν is also damped by a factor $m = \cos\psi$.

The light source

The pioneering work of Merkelo et al. [43] showed the first application of mode-locked lasers to phase fluorimetry in the field of photosynthesis. The high frequency (approx. 100 MHz) and high intensity (approx. 1 W) (obtained in this way) greatly increase the time resolution. In our laboratory, we have developed a new source of modulated light, easy to adapt to cryogenic phase fluorimetric measurements. This source is formed by an array of eight light-emitting diodes cooled to liquid nitrogen temperature. 100% light modulation is achieved by direct modulation of the driving current. A complete description of the system will be published in a forthcoming paper. The principal characteristics are: source diameter $\simeq$ 5.6 mm; divergency (half-angle) $\simeq$ 35°; optical power $\simeq$ 5–10 mW/cm^2; emission wavelength $\simeq$ 635 nm; full-width at half-maximum $\simeq$ 20 nm; modulation band width $\simeq$ 60 MHz.

The cryogenic setup

A concentrated suspension (approx. 200 μg/ml of total chlorophyll), but forming only one monolayer of cells (as can be checked under the microscope) is placed in a very thin cylindrical quartz cuvette of 0.1 mm depth and, after dark adaptation, quickly cooled by direct immersion in liquid nitrogen. A magazine containing 8 or 16 samples is introduced in the dark in the measuring Dewar vessel, which allows repetitive measurements and the averaging of results (Fig. 1). In the measuring vessel, the liquid N_2 level is detected by an electronic device and kept constant by automatic fill-

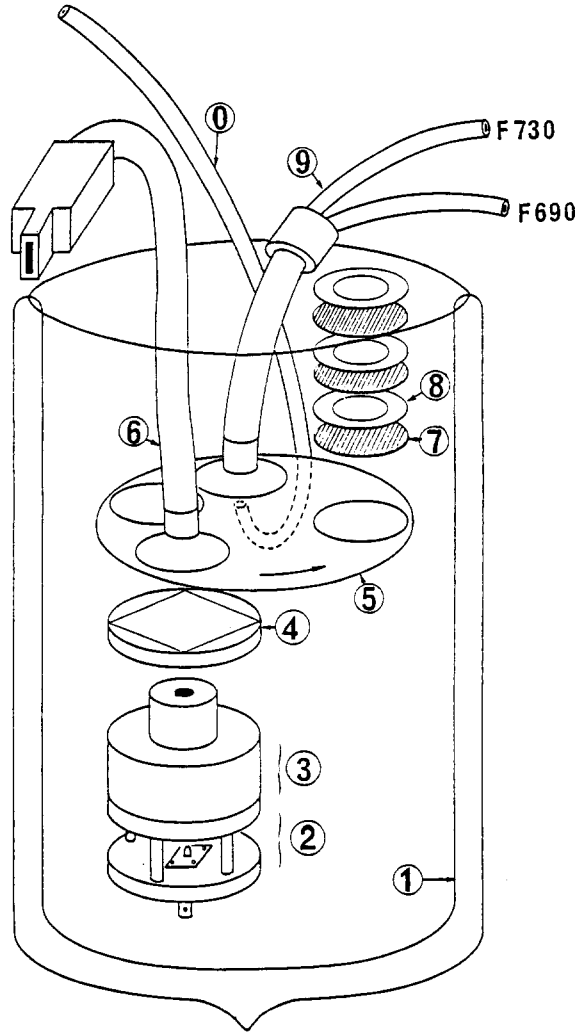

Fig. 1. Cryogenic set-up. (1) Dewar vessel; (2) light source (eight light-emitting diodes); (3) eight inputs, one output light pipe; (4) interference filter (50% peak transmission, peak 640 nm, full-width at half-maximum approx. 10 nm); (5) rotating wheel for sample commutation; (6) light pipe for fluorescence analysis; (7) sample spacer; (8) sample quartz cuvette, diameter 15 mm, depth 0.1 mm; (0) accessory light pipe for fluorescence kinetics measurements with an external light source; (9) two-arms light pipe for dual-wavelength analysis of fluorescence kinetics. The dark-adapted sample is first positioned in front of light pipe 0 for kinetics measurements and rotates further until it faces the light-emitting diode source for lifetime measurements (fluorescence kinetics are not reported here). 16 samples can be successively analyzed.

ing from an accessory reservoir. The measurements are made in the vapor phase. A heating resistor, placed at the bottom of the vessel, increases the natural evaporation and produces a small over-pressure to prevent ice formation. The temperature of the sample is approx. 80 ± 1 K. A light pipe collects the fluorescence which is analyzed through a Corning CS2-64 filter transmitting wavelengths greater than 665 nm, and a Jobin and Yvon M25 monochromator with a 4 nm band width; the transit time variations of the photomultiplier due to the different wavelengths analyzed have been discussed elsewhere [38,44]. In the experiments reported here these are second-order phenomena. The amplitude and phase shift spectra are recorded simultaneously on a multichannel analyser, averaged 8 or 16 times and transferred to a desk computer HP 9845. Fig. 2 shows a block diagram of the entire setup.

Analysis of performance

In spite of the precautions taken to ensure the reproducibility of the fluorescence intensity spectra, small fluctuations (±15%) persisted due to random ice formation. However, the fluctuations almost vanished after normalization of the spectra.

The overall reproducibility of the phase shift is within ±2%. This fact clearly points out that the fluorescence quantum yield of chlorophyll 'in vivo' at 80 K can be reproducible if the cooling process follows a strict protocol. Intensity differences are only produced by changes in the transmission properties of the samples.

In the phase fluorimetry method the time resolution is controlled by the modulation frequency and by phase detection sensitivity. In our instrument four frequencies can be selected; 7.25, 14.5, 29 and 58 MHz. For technical reasons, we have chosen to work at 29 MHz. With the assumed phase shift sensitivity of 0.1 degree, relative differences of 10 ps in lifetimes at two different wavelengths could be resolved. Absolute values are, however, accurate to within ±50 ps.

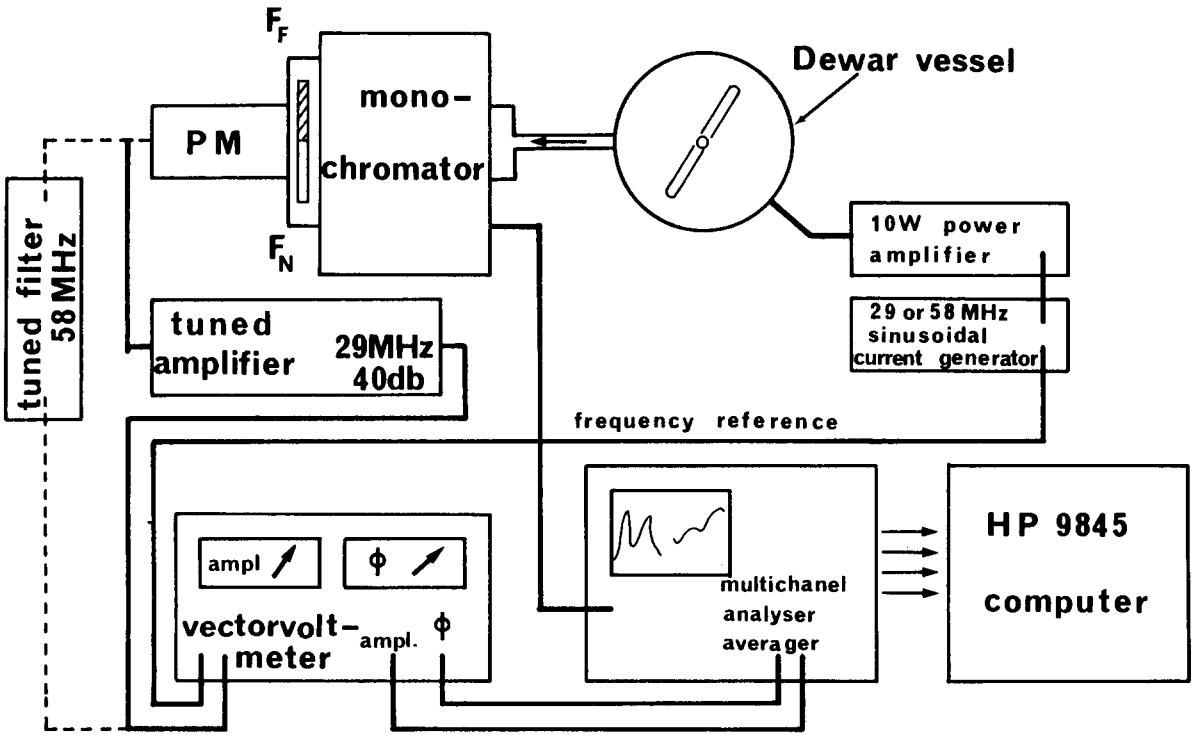

Fig. 2. Diagram of the experimental setup.

Results and Discussion

Fig. 3 shows both the fluorescence intensity and lifetime spectra obtained with four species of algae cooled after several minutes of dark adaptation. The spectra were recorded after stabilization of the fluorescence intensity at the F_{max} level under the modulated beam (i.e., all PS II traps closed). 16 consecutive spectra were averaged. No correction has been made for the wavelength-dependent sensitivity of the apparatus. It must be stated that the $\tau(\lambda)$ spectrum is not sensitive to these variations: the mean lifetime only depends on the ratio of the different emissions at a given wavelength, which is independent of transmission.

Two immediate observations can be made: (1) a comparison of the $\tau(\lambda)$ spectra in the four algae analyzed shows the same pattern of the mean lifetime spectra. This shape is a characteristic feature of low-temperature fluorescence spectra of photosynthetic material. (2) Lifetime is wavelength dependent: it varies from approx. 1.5 ns ($\tau(680)$) to 3.2 ns ($\tau(740)$) in *Chlorella* (Fig. 4a) (cf. 1.4 and 2.3 ns [27]). This variation arises from the overlapping of emission bands with different lifetimes. In the case where a single emitting species is present

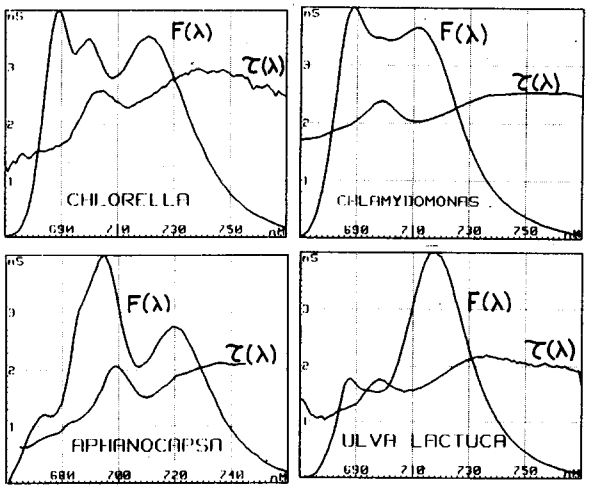

Fig. 3. Fluorescence intensity ($F(\lambda)$) and lifetime ($\tau_p(\lambda)$) spectra of four species of algae at 80 K. The samples have been frozen in the dark after dark adaptation. Modulation frequency, 29 MHz. In spite of the difference of $F(\lambda)$, the $\tau_p(\lambda)$ pattern remains constant. The $\tau_p(\lambda)$ variation arises from the overlapping of emission bands with different lifetimes.

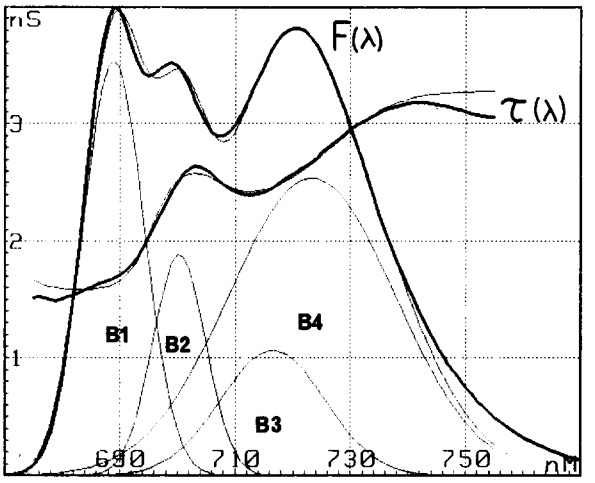

Fig. 4. The four-component Gaussian decomposition. Thick line: $F(\lambda)$ and $\tau_p(\lambda)$ spectra of *Chlorella* cells frozen in the dark down to 80 K. Modulation frequency, 29 MHz. Thin line: simultaneous fitting of the spectra by a four-component Gaussian model. Numerical values of parameters are listed in Table II. At least four components are necessary to describe the $\tau_p(\lambda)$ variations; however, multifrequency analysis suggests that lifetimes of B1 and B2 should be considered as mean values.

in the sample, one can expect to find a constant lifetime throughout the emission spectrum. We have checked this point with a solution of Chl *a* in ethanol at 20°C and found a flat $\tau(\lambda)$ curve with a lifetime of approx. 5 ns.

The obvious overlapping of emission bands leads us to the first conclusion that the lifetime values directly deduced from the phase delay measurements are ambiguous. To obtain a more pertinent description we have developed a Gaussian analysis of our spectra.

The problem of Gaussian decomposition of emission spectra has been attempted by several authors [6], but only on the basis of fluorescence intensity measurements; in this case an infinite number of solutions can formally describe the experimental spectra; the more individual components are considered, the more accurate is the fitting. We tried to fit simultaneously both the $F(\lambda)$ and $\tau(\lambda)$ spectra by the same elementary components. The calculations have been performed with a 9845 Hewlett Packard desk computer. Because $\tau(\lambda)$ and $F(\lambda)$ are obtained from independent information, the possible choice of unknown components is considerably restricted.

Nevertheless, we must make several assumptions.

(1) The elementary components are Gaussian:

$$F_i(\lambda) = F_i^{\circ} \exp\left[-(\lambda - \lambda_i)^2 4 \log 2/\sigma_i^2\right],$$

where F_i° is the maximum amplitude of the ith component, λ_i the wavelength of the peak position, and σ_i the full-width at half-maximum. It would be more correct to represent F_i as a Gaussian function of energy but in our case where the ratio σ_i/λ_i remains small, the difference is insignificant. The choice of a Gaussian shape for the elementary bands is a rough approximation which does not take into account the vibrational and of chlorophyll fluorescence.

(2) The number of components: at least four main elementary components are necessary to fit the $\tau(\lambda)$ spectra (Fig. 4). This is in contrast to the generally accepted opinion that three bands are sufficient (see, however, Ref. 4).

As we will see below, measurements at two different frequencies implies two additional bands in the short-wavelength range and a third minor one in the long-wavelength edge of the spectra.

(3) The elementary components are independent and decline according to an exponential law when excited with a short light pulse. In the frame of the phase fluorimetry theory [40,41], the observed a.c. signal at the frequency of modulation (29 MHz) is the vectorial sum of all elementary components:

$$\vec{F}(\lambda) = \Sigma_i \vec{F}_i(\lambda)$$

$\tilde{F}_i(\lambda) = F_i^{\circ}(\lambda) \cos \psi_i$ is the modulus of the ith component. $F_i^{\circ}(\lambda)$ is the amplitude of the ith component as it could be measured at a low modulation frequency; ψ_i is the phase delay between the fluorescence and the excitation; $\cos \psi_i$ the demodulation factor.

The phase delay ψ_i is related to the lifetime τ_i by the classical relation:

$$\tau_i = \tan \psi_i / 2\pi\nu \qquad (1)$$

The experimental parameter $\tilde{F}(\lambda)$ is the modulus of $\vec{F}(\lambda)$:

$$\tilde{F}(\lambda) = \left(\left(\Sigma F_i^{\circ}(\lambda) \cos^2\psi_i\right)^2 + \left(\Sigma_i F_i^{\circ}(\lambda) \cos \psi_i \cdot \sin \psi_i\right)^2\right)^{1/2} \qquad (2)$$

The experimental $\tau_p(\lambda)$ spectra are related to the overall phase delay by the relation:

$$\tau_p(\lambda) = \tan \psi / 2\pi\nu$$

$$= \left[\Sigma_i F_i^{\circ}(\lambda) \cos^2\psi_i \tan \psi_i / \Sigma_i F_i^{\circ}(\lambda) \cos^2\psi_i\right] / 2\pi\nu$$

$$= \Sigma_i F_i^{\circ}(\lambda) \cos^2\psi_i \cdot \tau_i / \Sigma_i F_i^{\circ}(\lambda) \cos^2\psi_i \qquad (3)$$

$\tau_p(\lambda)$ has the significance of a mean lifetime in which amplitude of the components are $F_i^{\circ}(\lambda) \cos^2\psi_i$. The relations (1) and (2) contains $4 \times i$ unknown parameters (F_i°, λ_i, σ_i and τ_i for the i components) which can be adjusted by a least-square programme.

The four-component decomposition

The $\tau_p(\lambda)$ spectrum suggests that at least four components are required to describe its main variations. Fig. 4 and Table II show the result of the Gaussian decomposition (in the 675–740 nm wavelength range). The model seems to fit correctly the experimental data except at the two edges: for $\lambda > 740$ nm a supplementary component must be added to explain the $\tau_p(\lambda)$ decrease, and around 685 nm where the slope of the experimental $\tau_p(\lambda)$ spectra cannot be explained by only one component, as does the model. In this four-component model the lifetime values of elementary bands are very close to the values directly deduced from the experimental data as we can see in Table II, except for the B3 component which is obtained only by Gaussian decomposition. To be a satisfactory fit, such a decomposition must be independent of the frequency of modulation at which the measurements are made. Preliminary

TABLE II

VALUES OF GAUSSIAN PARAMETERS OF A FOUR-COMPONENT DECOMPOSITION

Band	$F_i^{\circ} \cos^2\psi_i$ (arbitrary units)	F_i° (% of the band)	λ_i (nm)	σ_i (nm)	τ_i (ns)
B1	3.54	1	688.9	12.4	1.54
B2	1.89	0.61	700.3	10.8	2.64
B3	1.07	0.29	716.5	21.2	0.72
B4	2.54	0.9	723.3	33.8	3.28

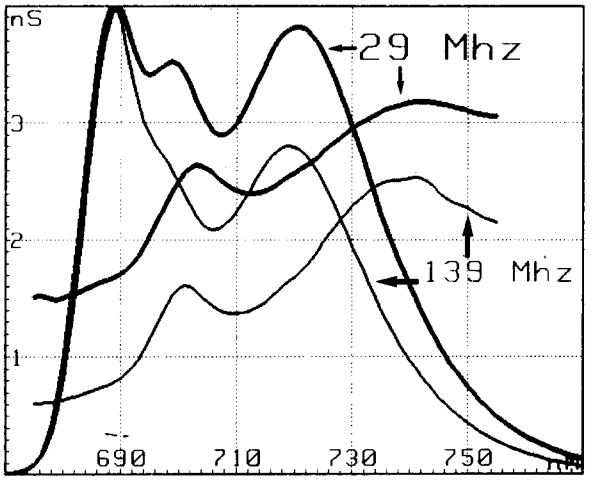

Fig. 5. Spectra at two different frequencies. The same sample of *Chlorella* cells has been analyzed under the same conditions at two different frequencies: 29 and 139 MHz. The amplitude spectra have been normalized at 688 nm. Lower values for $\tau_p^{139}(\lambda)$ are due to the relative increase in the short-lifetime components. Note the strong frequency effect on lifetime for $\lambda < 710$ nm.

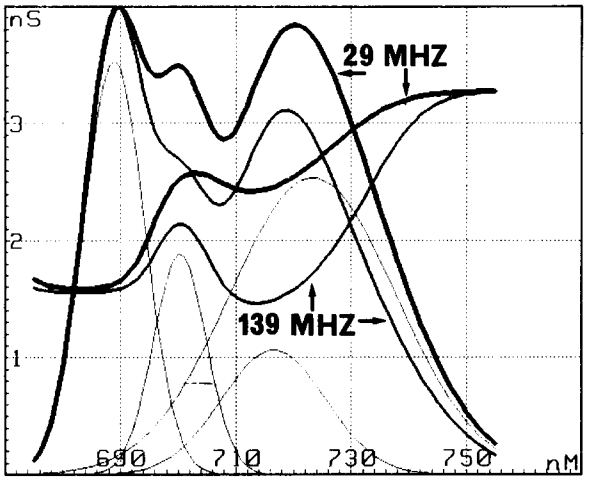

Fig. 6. Effect of the modulation frequency on the four-component model. The theoretical model used to fit the experimental data of Fig. 4 and Table II was recomputed at 139 MHz and normalized. Note the absence of frequency effect for $\lambda < 710$ nm.

measurements at 139 MHz * clearly show that it is not the case.

Fig. 5 compares the spectra obtained at 139 MHz with those obtained at 29 MHz; the $\tau_p(\lambda)$ pattern is conserved but the absolute values of lifetimes are decreased by about 1 ns. The shape of $F(\lambda)$ is also strongly affected by the new modulation frequency. From Eqns. 1–3 we can predict that the increase in ν must result in a relative increase in the short-lifetime components which leads to the decrease of the measured $\tau_p(\lambda)$ spectrum in the spectral range where an overlapping of different emission bands takes place. Any change in $\tau_p(\lambda)$ must be measured at wavelengths where only one emission band is predominant. Fig. 6 represents the four-component model of Fig. 4 recalculated at 139 MHz. It is obvious that the four-component model is incomplete and cannot explain the two frequency results. The overall decrease in $\tau_p^{139}(\lambda)$ compared to $\tau_p^{29}(\lambda)$ means that the overlapping of emission bands exists in the entire region of the spectrum (at least between 675 and 755 nm). The simplest hypothesis of four Gaussian bands required to take into account low-temperature fluorescence spectra fails also in the case of spinach chloroplasts, where we find the same kind of results in a more complete two-frequency analysis (to be published).

The seven-component decomposition

To take into account our frequency effect, two additional bands with a lifetime about 4–6 ns must be added in the $\lambda < 740$ nm range and a third one with a short lifetime in the $\lambda > 740$ nm range; all these bands are necessary for an accurate description of our data. Fig. 7 and Table III show the Gaussian decomposition with seven components obtained by a simultaneous fitting, by the least-squares program, of both $F(\lambda)$ and $\tau(\lambda)$ spectra obtained at the two frequencies.

The findings by successive iterations of such a set of seven components describing the experimental spectra and their stability under the modulation frequency variation are not quite unique (i.e., depending on the initial conditions, a slightly different solution can be found by the computing program). Nevertheless, we believe that within 20%

* The 139 MHz modulation frequency was obtained with a mode-locked dye laser emitting at the same wavelength as that our diode system (635 nm). The experimental setup will be described elsewhere.

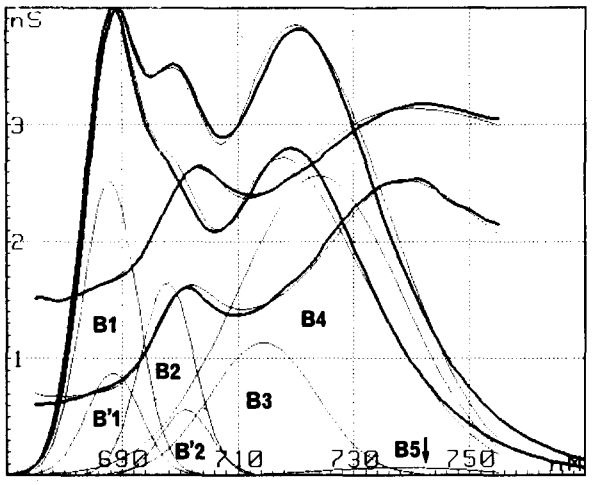

Fig. 7. Simultaneous fitting of $\tau_p^{29}(\lambda)$, $F^{29}(\lambda)$, $\tau_p^{139}(\lambda)$, $F^{139}(\lambda)$ by a seven-component model. Thick line: experimental data at 29 and 139 MHz. Thin line: seven-component model. Long-lifetime components B'1 and B'2 in the short-wavelength range of the spectra are required to take into account the two-frequency measurements. Numerical values of the components are listed in Table III.

margin, realistic lifetime values of the main components emitting at low temperature, are obtained.

Assignment of fluorescent bands

The origin and significance of the emission bands that can occur at low temperature are not well established yet and can be only explained in a tentative way (see, e.g., Refs. 7 and 46).

TABLE III

VALUES OF GAUSSIAN PARAMETERS OF A SEVEN-COMPONENT DECOMPOSITION

Band	$F_i^\circ \cos^2\psi_i$ (arbitrary units)	F_i° (% of the greater band)	λ_i (nm)	σ_i (nm)	τ_i (ns)
B'1	2.53	0.73	687.9	11	0.53
B''1	0.88	0.44	688.5	11	4.79
B'2	1.65	0.51	697.8	11	1.46
B''2	0.56	0.33	700.1	10.3	5.61
B3	1.24	0.36	714.4	21.6	0.72
B4	2.56	1	724	33.6	3.32
B5	0.07	0.02	738.1	30.5	0.41

B1 and B2 bands

The B1 emission located at approx. 689 nm on *Chlorella* corresponds to the F-685 nm band of chloroplasts of green plants. This band exhibits a 2–3-fold increase when the PS II reaction center becomes closed. It has been shown by Rijgersberg et al. [7] that this band is still present in a barley mutant lacking LHC (light-harvesting Chl *a*/*b*-protein complex). This band seems associated with the PS II Chl *a* antenna rather than the LHC, as it has been first proposed by Strasser and Butler [19]. When integrated in the thylakoid membrane, the emission of the LHC seems associated with a weak band near 680 nm only visible at temperatures lower than 77 K [7]. This band disappears in the barley mutant deficient in LHC.

The B2 band follows the same fluorescence induction kinetics as does B1. It has been shown by Satoh [47] that F-695 (which corresponds to the B2 emission in *Chlorella*) is still present in the fluorescence emission of the PS II Chl *a*-protein complex. However, a shoulder at 695 nm is also seen in some preparations of isolated LHC which is correlated with the aggregation state [48,49].

In the present work, it has been possible to evidence the strong heterogeneity of the B1 and B2 bands, each containing a main short-lived emission (B'1 ≃ 0.5 ns; B'2 ≃ 1.5 ns) and a long-lived emission (B''1 ≃ 4.8 ns; B''2 ≃ 5.6 ns), the lifetime of which is close to that of chlorophyll in organic solvent.

We propose to attribute B'1 and B'2 to the PS II Chl *a*-protein complex connected to the reaction center. The lifetimes of these bands deduced from our two-frequency analysis are similar to or smaller than those observed at the F_{max} level on *Chlorella* cells at room temperature: mean lifetime approx. 1.8 ns [42,50]. Thus, the quantum yield $\phi = \tau/\tau_0$ (τ_0 natural lifetime) for B'1 and B'2 is similar to that at room temperature. The obvious increase in fluorescence intensity in the spectral range $\lambda < 710$ nm when the temperature is lowered from 300 to 77 K could be due essentially to the appearance of B''1 and B''2 bands.

B''1 and B''2 bands

The existence of long-lifetime emissions in the short-wavelength range of the spectra ($\lambda < 710$ nm) was first reported by Hervo et al. [28] in

lifetime measurements by the single-photon-counting technique at low temperature on chloroplasts. Two different hypotheses can be proposed to explain their origin. (1) Disconnected chlorophyll: at cryogenic temperatures some subsets of chlorophyll may lose their connection with the main functional antenna. Thus, a new emission could appear, characterized by a longer lifetime and without major changes in the wavelength emission. Due to its reduced size, the lifetime of the functional antenna tends to be shortened. (2) Delayed fluorescence can also be considered as a possible mechanism to produce long-lifetime fluorescence emission. Because the primary quinone acceptor of PS II is reduced under illumination at 77 K, charge recombination in reaction centers could reintroduce excited singlet chlorophyll states in the antenna. The spectral characteristics of such delayed emission must be similar to those of the directly excited fluorescence, except for the lifetime parameter that must be lengthened by the time needed for charge pair generation and recombination. Several authors have recently proposed this type of mechanism in experiments with bacterial reaction centers [51–54].

B3 band

This band cannot be resolved usually in the fluorescence amplitude spectra: however, data reported by Cho and Govindjee [4], showing a shoulder near 717 nm in the fluorescence spectrum of *Chlorella* cells at 77 K, are in good agreement with our observations. The $\tau(\lambda)$ spectrum allow us to provide evidence for this band in all photosynthetic material that we have analysed. The lifetime value for this band deduced from the Gaussian decomposition is approx. 0.8 ns, which is not very different from the value obtained for B'1: one can suppose that B3 is a vibrational band of B'1. A possible argument against this assumption is that B3 can also be found in isolated PS I subchloroplast particles [55].

Another argument leading to the same conclusion has been obtained by comparison between a mutant of *C. reinhardii,* lacking P-700 (but still having a PS I antenna [56]) and the wild type: we found a specific increase in both relative amplitude and lifetime of B3 in the case of the mutant. Out interpretation is that B3 can be identified with the antenna directly associated with P-700. The fluorescence quantum yield of B3 is ordinarily low due to the efficient energy transfer to P-700 but in the absence of the natural energy sink (mutant case). The quantum yield of B3 is dramatically increased [42].

B4 band

Approx. 50% of the low-temperature fluorescence increase comes from this band which is very temperature sensitive between room and liquid nitrogen temperature. It has been proposed by Butler [23] that B4 emanates from a small amount of a long-wavelength form of chlorophyll (C-705) which acts as a trap of excitation energy in the PS I antenna. This long-wavelength emission can also be seen in subchloroplast PS I particles containing approx. 110 Chl/P-700 [55]. It disappears in a further purification step leading to a more enriched preparation with about 60 Chl/P-700. To our knowledge, there is no definitive argument to conclude whether B4 is emitted by a small amount of Chl *a* molecules (C-705 hypothesis) or whether it comes from an antenna pigment array less tightly coupled to P-700 than B3.

B5 band

In spite of its small intensity, this component is formally required to describe both the decrease in the $\tau_p(\lambda)$ spectra for $\lambda > 740$ nm and the frequency effect on lifetime in the same wavelength range. These two observations concerning the B5 band are nonexistent in chloroplasts. Investigations of the polarization of fluorescence in magnetically oriented material at 77 K made by Vasin and Vekhoturov [57] also point out the same difference in a long-wavelength component between *Chlorella* cells and chloroplasts. More generally, the polarization ratio analysis carried out by these authors reveal almost the same components as our lifetime analysis.

References

1 Tollin, G. and Calvin, M. (1957) Proc. Natl. Acad. Sci. U.S.A. 43, 895–908
2 Brody, S.S. (1958) Science 128, 838–839
3 Butler, W.L. and Kitajima, M. (1975) Biochim. Biophys. Acta 396, 72–85
4 Cho, F. and Govindjee (1970) Biochim. Biophys. Acta 216, 139–150

5 Harnischfeger, G. (1977) Adv. Biol. Res. 5, 1–51
6 Litvin, F.F., Sineshchekov, V.A. and Shubin, V.V. (1976) Biofizika 21, 669–675
7 Rijgersberg, C.P., Amesz, J., Thielen, A.P.G.M. and Swager, J.A. (1979) Biochim. Biophys. Acta 545, 473–482
8 Govindjee, Papageorgiou, G. and Rabinowitch, E. (1967) in Fluorescence Theory, Instrumentation and Practice (Guilbault, G.G., ed.), pp. 511–564, M. Dekker, New York
9 Papageorgiou, G. (1975) in Bioenergetics of Photosynthesis (Govindjee, ed.), pp. 319–371, Academic Press, New York
10 Lavorel, J. and Etienne, A.L. (1977) in Primary Processes in Photosynthesis (Barber, J., ed.), pp. 203–268, Elsevier, Amsterdam
11 Paillotin, G. (1974) Ph.D. Thesis, Paris-Sud, Orsay
12 Govindjee and Yang, L. (1966) J. Gen. Physiol. 49, 763–780
13 Butler, W.L. (1973) Acc. Chem. Res. 6, 177–184
14 Murata, N., Itoh, S. and Okada, M. (1973) Biochim. Biophys. Acta 325, 463–471
15 Ley, A.C. and Butler, W.L. (1976) Proc. Natl. Acad. Sci. U.S.a. 73, 3957–3960
16 Satoh, K., Strasser, R. and Butler, W.L. (1976) Biochim. Biophys. Acta 440, 337–345
17 Butler, W.L. and Strasser, R.J. (1977) Biochim. Biophys. Acta 462, 290–294
19 Strasser, R.J. and Butler, W.L. (1977) Biochim. Biophys. Acta 462, 295–306
20 Strasser, R.J. and Butler, W.L. (1977) Biochim. Biophys. Acta 462, 307–313
21 Butler, W.L. and Strasser, R.J. (1977) Proc. Natl. Acad. Sci. U.S.A. 74, 3382–3385
22 Satoh, K. and Butler, W.L. (1978) Biochim. Biophys. Acta 502, 103–110
23 Butler, W.L. (1978) Annu. Rev. Plant Physiol. 29, 345–378
24 Wong, D., Merkelo, H. and Govindjee (1981) Photochem. Photobiol. 33, 97–101
25 Wong, D. and Govindjee (1981) Photochem. Photobiol. 33, 103–108
26 Butler, W.L. and Norris, H.K. (1963) Biochim. Biophys. Acta 66, 72–77
27 Mar, T., Govindjee, Sighal, G.S. and Merkelo, H. (1972) Biophys. J. 12, 797–808
28 Hervo, G., Paillotin, G., Thiery, J. and Breuze, G. (1975) J. Chim. Phys. 72, 701–706
29 Harris, L., Porter, G., Synowiec, J.A., Tredwell, C.J. and Barber, J. (1976) Biochim. Biophys. Acta 449, 329–339
30 Searle, G.F.W., Barber, J., Harris, L., Porter, G. and Tredwell, C.J. (1977) Biochim. Biophys. Acta 459, 390–401
31 Porter, G., Synowiec, J.A. and Tredwell, C.J. (1977) Biochim. Biophys. Acta 459, 329–336
32 Yu, W., Pellegrino, F. and Alfano, R.R. (1977) Biochim. Biophys. Acta 460, 171–181
33 Geacintov, N.E., Breton, J., Swenberg, C., Campillo, A.J., Hyer, R. and Shapiro, S.L. (1977) Biochim. Biophys. Acta 461, 306–312
34 Campillo, A.J., Shapiro, S.L., Geacintov, N.E. and Swenberg, C.E. (1977) FEBS Lett. 83, 316–320
35 Rubin, L.B. and Rubin, A.B. (1978) Biophys. J. 6, 347–359
36 Butler, W.L., Tredwell, C.J., Malkin, R. and Barber, J. (1979) Biochim. Biophys. Acta 545, 309–315
37 Wong, D., Merkelo, H. and Govindjee (1979) FEBS Lett. 104, 223–226
38 Moya, I. (1974) Biochim. Biophys. Acta 368, 214–227
39 Herdman, M., Delaney, S.F. and Carr, N.G. (1973) J. Gen. Microbiol. 79, 233–237
40 Tumerman, L.A. (1941) J. Physics 4, 151–166
41 Bailey, E.A. and Rollefson, G.K. (1953) J. Chem. Phys. 21, 1315–1322
42 Moya, I. (1979) Ph.D. Thesis, Paris-Sud, Orsay
43 Merkelo,H., Hartman, S.R., Mar, J., Singhal, G.S. and Govindjee (1969) Science 164, 301–302
44 Muller, A., Lumry, R. and Walker, S. (1969) Photochem. Photobiol. 9, 113–120
45 Tumerman, L.A. and Sorokin, E.M. (1967) Mol. Biol. 1, 628–638
46 Gasanov, R., Abilov, Z.K., Gazanchyan, R.M., Kurbonara, U.M., Khanna, R. and Govindjee (1979) Z. Pflanzenphysiol. 95, 149–169
47 Satoh, K. (1980) FEBS Lett. 110, 53–56
48 Mullet, J.E. and Arntzen, C.J. (1980) Biochim. Biophys. Acta 589, 100–107
49 Larkum, A.W.D. and Anderson, J.M. (1982) Biochim. Biophys. Acta 679, 410–421
50 Briantais, J.M., Merkelo, H. and Govindjee (1972) Photosynthetica 6, 133–141
51 Godik, V.I. and Borisov, A.Yu (1979) Biochim. Biophys. Acta 548, 296–308
52 Godik, V.I. and Borisov, A., Yu (1980) Biochim. Biophys. Acta 590, 182–193
53 Shuvalov, V.A. and Klimov, V.V. (1976) Biochim. Biophys. Acta 440, 587–599
54 Shuvalov, V.A., Klimov, V.V., Dolan, E., Parson, W.W. and Ke, B. (1980) FEBS Lett. 118, 279–282
55 Moya, I., Mullet, J.E., Briantais, J.M. and Garcia, R. (1981) in Proceedings of the 5th International Congress on Photosynthesis (Akoyunoglou, G., ed.), pp. 163–171, Balaban International Science Services, Philadelpha
56 Garnier, J. and Maroc, J. (1972) Biochim. Biophys. Acta 283, 100–114
57 Vasin, Yu, A. and Vekhoturov, V.N. (1979) Biophysics 24, 269–273